doi:10.1093/brain/aws210 Brain 2012: 135; 2817–2825 | 2817

BRAIN
A JOURNAL OF NEUROLOGY

Decreased carbon-11-flumazenil binding in early Alzheimer's disease

Belen Pascual,[1,2,*] Elena Prieto,[3] Javier Arbizu,[2,3] Josep M. Marti-Climent,[2,3] Ivan Peñuelas,[3] Gemma Quincoces,[3] Rosina Zarauza,[4] Sabina Pappatà[5] and Joseph C. Masdeu[1,2,†]

1 Neuroscience Division, Centre for Applied Medical Research, University of Navarra, Pamplona, 31008, Spain
2 CIBERNED, Pamplona, 31008, Spain
3 Department of Nuclear Medicine, University of Navarra, Pamplona, 31008, Spain
4 Department of Anaesthesiology and Critical Care, University of Navarra, Pamplona, 31008, Spain
5 Institute of Biostructure and Bioimaging, Consiglio Nazionale delle Ricerche, Naples, 80131, Italy

*Present address: Frontotemporal Dementia Unit, Athinoula A. Martinos Centre for Biomedical Imaging, Department of Neurology, Massachusetts General Hospital; and Department of Neurology, Harvard Medical School, Charlestown, Massachusetts 02129, USA
†Present address: Section on Integrative Neuroimaging, Clinical Brain Disorders Branch, Intramural Research Program, National Institutes of Health, Bethesda, MD 20892, USA

Correspondence to: Belen Pascual, Ph.D.,
Frontotemporal Dementia Unit,
Athinoula A. Martinos Centre for Biomedical Imaging,
Massachusetts General Hospital and Harvard Medical School,
149 13th Street, 149-2691,
Charlestown, MA 02129, USA
E-mail: belen@nmr.mgh.harvard.edu

Neuronal loss in Alzheimer's disease, a better correlate of cognitive impairment than amyloid deposition, is currently gauged by the degree of regional atrophy. However, functional markers, such as $GABA_A$ receptor density, a marker of neuronal integrity, could be more sensitive. In post-mortem hippocampus, $GABA_A$ messenger RNA expression is reduced even in mild cognitive impairment. We measured whole-brain $GABA_A$ binding potential *in vivo* using [^{11}C]-flumazenil positron emission tomography and compared $GABA_A$ binding with metabolic and volumetric measurements. For this purpose, we studied 12 subjects, six patients with early Alzheimer's disease and six healthy controls, with [^{11}C]-flumazenil and [^{18}F]-fluorodeoxyglucose positron emission tomography, as well as with high-resolution magnetic resonance imaging. Data were evaluated with both voxel-based parametric methods and volume of interest methods. We found that in early Alzheimer's disease, with voxel-based analysis, [^{11}C]-flumazenil binding was decreased in infero-medial temporal cortex, retrosplenial cortex and posterior perisylvian regions. Inter-group differences reached corrected significance when using an arterial input function. Metabolism measured with positron emission tomography and volumetric measurements obtained with magnetic resonance imaging showed changes in regions affected in early Alzheimer's disease, but, unlike with [^{11}C]-flumazenil binding and probably due to sample size, the voxel-based findings failed to reach corrected significance in any region of the brain. With volume of interest analysis, hippocampi and posterior cingulate gyrus showed decreased [^{11}C]-flumazenil binding. In addition, [^{11}C]-flumazenil hippocampal binding correlated with memory performance. Remarkably, [^{11}C]-flumazenil binding was decreased precisely in the regions showing the greatest degree of neuronal loss in post-mortem studies of early Alzheimer's disease. From these data, we conclude that [^{11}C]-flumazenil binding could be a useful marker of neuronal loss in early Alzheimer's disease.

Keywords: Alzheimer's disease; flumazenil PET; MRI; $GABA_A$ receptors

Received March 20, 2012. Revised June 12, 2012. Accepted June 21, 2012

Introduction

In brains of patients with Alzheimer's disease with the mildest clinically detectable dementia (Clinical Dementia Rating scale = 0.5), a 32% loss of neurons has already occurred in the entorhinal cortex (Gomez-Isla *et al.*, 1996). Neuronal loss spreads as the disease progresses and correlates better than amyloid deposition with the degree of clinical worsening (Crystal *et al.*, 1988; Gomez-Isla *et al.*, 1996; Giannakopoulos *et al.*, 2003). Regional neuronal loss can be gauged by the degree of atrophy, currently used as a neuroimaging marker of neuronal loss (Killiany *et al.*, 2000; Chetelat *et al.*, 2010). It is possible, however, that imaging of receptors ubiquitous in neurons, such as the $GABA_A$ receptor (Kisvarday *et al.*, 1990), could be more sensitive than atrophy to neuronal loss in Alzheimer's disease. In post-mortem hippocampus, a decreased expression of the $GABA_A$ messenger RNA has been described even in mild cognitive impairment (Rissman *et al.*, 2004). Regional $GABA_A$ receptor availability can be quantified *in vivo* with [^{11}C]-flumazenil PET, which has been reported to be more specific than diffusion-weighted MRI for the detection of neuronal loss in stroke (Heiss *et al.*, 2004). In contrast, a single patient study and two previous series using [^{11}C]-flumazenil in Alzheimer's disease have been negative (Sedvall *et al.*, 1987; Meyer *et al.*, 1995; Ohyama *et al.*, 1999). The study by Meyer *et al*. (1995) included five patients with mild or early Alzheimer's disease (mean Mini-Mental State Examination = 22) and six healthy controls. Ohyama *et al*. (1999) studied five patients with probable Alzheimer's disease and five healthy controls. Partly because lateral temporoparietal association cortex shows the greatest metabolic loss in Alzheimer's disease, these PET studies focused on a comparison of metabolism or regional cerebral blood flow with [^{11}C]-flumazenil binding in these regions. However, these are not the regions where the greatest neuronal loss has been detected in post-mortem studies (Brun and Englund, 1981). Additionally, the relationship between atrophy and metabolism is complex, with areas, such as the hippocampus, where there is atrophy but relatively preserved metabolism and others with marked metabolic decline but little atrophy (Chetelat *et al.*, 2008). This is not surprising because metabolism reflects synaptic activity (Rocher *et al.*, 2003); metabolic loss in a region may simply reflect neuronal loss in the region home to the neurons projecting to the metabolically impaired region. Lateral parietotemporal association cortex receives a heavy projection from the medial temporal region (Lavenex *et al.*, 2002; Munoz and Insausti, 2005), with marked neuronal loss in Alzheimer's disease (Gomez-Isla *et al.*, 1996, 1997). None of the previous [^{11}C]-flumazenil studies in Alzheimer's disease were performed using voxel-wise comparisons, partial volume correction or normalization starting with PET co-registration to native MRI. We postulated that more recent imaging methods could facilitate detecting $GABA_A$-binding abnormalities in early Alzheimer's disease. We chose a small sample size to determine whether [^{11}C]-flumazenil PET could separate patients with early Alzheimer's disease from healthy controls when the power of the voxel-based analysis was too low to separate these two groups based on two Alzheimer's disease neuroimaging markers, namely grey matter atrophy on MRI or reduced metabolism on [^{18}F]-fluorodeoxyglucose PET (Chen *et al.*, 2011).

Table 1 Demographics and results of dementia screening tests

Variable	Alzheimer's disease	Healthy controls
Number of subjects	6	6
Gender (female)	3	4
Age (years)	78.0 (6.1)	78.2 (3.2)
Years of education	10.0 (3.4)	10.0 (3.4)
Dementia screening		
Clinical dementia rating		
Memory (range: 0–3)	1.1 (0.5)*	0
Sum of boxes (range: 0–18)	4.2 (3.6)*	0
Mini-Mental State Examination (range: 0–30)	21.2 (5.9)*	28.8 (0.7)
DemTect (range 0–19) (Kalbe *et al.*, 2004)	8.0 (2.3)*	18.2 (1.2)

Data are presented as means, with standard deviations in parentheses.
*Worse performance than healthy controls, $P < 0.05$.

Materials and methods

Participants

Twelve participants, divided into two groups (Alzheimer's disease and healthy controls) of six participants each, were studied with neuropsychological testing, structural MRI and PET with [^{18}F]-fluorodeoxyglucose PET and [^{11}C]-flumazenil, a $GABA_A$ receptor antagonist. Participants in the two groups had similar age, sex and educational level (Table 1). Patients with Alzheimer's disease met National Institute of Neurological and Communication Disorders and Stroke - Alzheimer Disease and Related Disorders Association (NINCDS-ADRDA) criteria (McKhann *et al.*, 1984) for the diagnosis of probable Alzheimer's disease but with a mild degree of cognitive impairment (mean Mini-Mental State Examination score was 21.2). Other neurological or psychiatric disorders were excluded in both patients with Alzheimer's disease and controls by a thorough medical and neurological evaluation, including standard biochemical and haematological studies. Because both groups had served as controls for another study (Pascual *et al.*, 2010), comparing them to patients with microvascular disease, the presence of vascular lesions, including white matter changes visible on T_1-weighted images or more than punctate hyperintensities on T_2-weighted images, was carefully excluded by MRI. To facilitate sleep, one patient and one healthy control were taking a similar dose of lormetazepam, which in both cases was discontinued 1 week before the PET procedure. Two patients were taking donepezil, also discontinued 1 week before undergoing PET. The study had been approved by the local Ethics Committee following Declaration of Helsinki guidelines for the study of human subjects. All subjects were fully instructed on the experimental procedures and provided written, informed consent.

Neuropsychological testing

The tests performed are listed in Table 2. They were obtained according to standard procedures and were analysed using SPSS Version 17 (2006). Due to the small sample size, comparisons between patients

Table 2 Neuropsychological testing performance and its correlation with [^{11}C]-flumazenil hippocampal binding

Test	Performance Alzheimer disease patients	Performance Healthy controls	Correlation (*r*) with [^{11}C]-flumazenil hippocampal binding	
			Left	Right
Cognitive domains				
Memory				
RAVLT				
First five trials	22.6 (7.2)*	40.3 (9.1)	0.834*	0.569
Immediate recall	2.4 (1.7)	8.7 (5.1)	0.731*	0.460
Delayed recall	1.2 (1.8)*	8.3 (5.1)	0.763**	0.558
Recognition	8.8 (5.8)	13.3 (1.5)	0.497	0.534
FCSRT	44.0 (25.0)*	83.3 (4.5)	0.620*	0.524
Logical memory				
Immediate recall	10.0 (6.0)*	28.5 (9.0)	0.825*	0.620*
Delayed recall	2.4 (2.8)	15.3 (9.9)	0.752**	0.679*
Recognition	10.4 (6.5)	19.0 (7.0)	0.764**	0.682*
Rey complex figure, recall	4.2 (4.0)*	18.4 (5.7)	0.682*	0.491
Language				
Boston naming test	39.2 (9.6)	50.2 (5.6)	0.639	0.694*
Verbal fluency (named in 1')				
Animals	11.0 (3.6)*	18.0 (4.0)	0.627*	0.471
Words starting with letter 'P'	12.8 (6.3)	16.8 (6.2)	0.223	0.355
Token test	17.2 (3.6)	19.5 (0.5)	0.616*	0.665*
Visuospatial function				
Rey complex figure, copy	22.7 (13.0)*	33.7 (2.1)	0.673*	0.426
Visual span backwards	4.0 (1.9)	6.8 (2.6)	0.472	0.306
Executive function, attention and speed of processing				
Trail making test				
Part A	107.4 (108.6)	70.7 (26.2)	−0.210	−0.260
Part B	265.8 (76.5)	147.0 (89.5)	−0.582	−0.458
Stroop test: WC	23.8 (15.8)	29.3 (6.0)	−0.078	0.164
Mental control WAIS-R	17.0 (7.6)	24.5 (5.2)	0.607*	0.457
Digit span forward, backwards	10.0 (3.4)	14.7 (3.4)	0.425	0.315
Fluctuation inventory scale	0	0	0	0
Other domains				
IADL	19.2 (6.8)*	8.3 (0.8)	−0.849**	−0.658*
Geriatric depression scale	12.4 (4.1)	5.2 (4.4)	−0.687*	−0.407
Neuropsychiatric inventory	3.6 (2.9)	1.7 (1.9)	−0.479	−0.074

Performance data are presented as means, with standard deviations in parentheses.
FCSRT = free and cued selective reminding test, pictures version; IADL = instrumental activities of daily living scale; RAVLT = rey auditory verbal learning test; WAIS-R = Wechsler adult intelligence scale-revised; WC = word-color.
*$P < 0.05$; **$P < 0.01$.

with Alzheimer's disease and healthy controls were performed using the non-parametric Mann–Whitney *U* test. Alpha was set at 0.05 for all analyses. Spearman simple correlations were conducted across the entire sample to determine the relationship between neuropsychological test performance and hippocampal [^{11}C]-flumazenil binding.

Magnetic resonance imaging data acquisition and processing

MRI was obtained for all participants on the same 3 T Siemens Trio scanner (Siemens Medical Solutions), including T_1-weighted structural images acquired using a 3D MP-RAGE sequence, with imaging parameters: resolution = 1 × 1 × 1.1 mm^3, field of view = 240 × 256 mm^2, 160 sagittal slices, repetition time/echo time/nversion time = 2250/900/2.96 ms, flip angle = 9°, bandwidth = 230 Hz/pixel. Whole-brain cortical thickness and hippocampal volume were determined using FreeSurfer software (Athinoula Martinos Centre for Biomedical Imaging). Voxel-based morphometry was performed with SPM8 software (Wellcome Department of Imaging Neuroscience, University College of London), using a fast diffeomorphic registration algorithm (DARTEL; Ashburner 2007). Details of the MRI methods are provided in the online Supplementary material.

[^{18}F]-Fluorodeoxyglucose positron emission tomography data acquisition and processing

Brain metabolism was measured with [^{18}F]-fluorodeoxyglucose PET using standard acquisition and processing methods (Supplementary material).

[^{11}C]-Flumazenil positron emission tomography data acquisition and processing

$GABA_A$ binding was measured with [^{11}C]-flumazenil PET using an ECAT EXACT HR+ (Siemens/CTI) scanner with a nominal resolution of 4.5 mm but a measured resolution of 7.3 mm (Prieto *et al.*, 2010). Subject motion was minimized with individually fitted thermoplastic masks. Following a transmission scan obtained using three ^{68}Ge sources and after the bolus injection of 659.71 (±136.16) MBq (17.83 ± 3.68 mCi) of [^{11}C]-flumazenil, a set of 19 sequential 3D PET frames of the entire brain were obtained over a period of 60 min, according to the following protocol: 4 × 30 s, 3 × 60 s, 2 × 150 s and 10 × 300 s. Arterial blood samples were drawn from the radial artery during the dynamic emission scans, for a total of 21 blood samples (intervals: 8 × 15 s, 3 × 60, 2 × 150 and 8 × 300 s). The sampled blood was processed to obtain arterial plasma input function for modelling. Using a procedure that provides reliable findings for [^{11}C]-flumazenil PET (Okazawa *et al.*, 2004), metabolites were not measured but were calculated as described by Okazawa *et al.* (2004), and plasma input function corrected accordingly. The radioactivity measured in the PET scans and blood samples was corrected for decay to the starting point of each scan.

Voxel-based parametric images of [^{11}C]-flumazenil volume of distribution (V_T) were computed with PMOD software (PMOD Technologies) using the graphic plot method of Logan. The slope of the graphical plot was calculated from 15 to 60 min, representing the volume of distribution (Innis *et al.*, 2007), which is here simply

called 'binding'. For the voxel-based analysis, PET studies were spatially normalized with SPM8 after individual PET and structural MRI studies had been co-registered in native space. Using Statistical Parametric Mapping 8 (SPM8), we analysed [^{11}C]-flumazenil binding, both for the whole brain and for a volume of interest including the entire temporal lobes of both hemispheres as the medial temporal regions have previously been identified as bearing marked neuronal loss in early Alzheimer's disease (Gomez-Isla *et al.*, 1996).

For volume of interest analysis, [^{11}C]-flumazenil parametric images of each subject were processed and corrected for partial volume effects using the method of Rousset *et al.* (1998) implemented in PVElab (pvelab@nru.dk) (Quarantelli *et al.*, 2004). The point-spread function to perform partial volume correction was calculated by determining the true resolution of the PET camera (Prieto *et al.*, 2010). Thus, a full-width at half-maximum of 7.3 mm was used for this purpose. Individual PET images were co-registered to high-resolution native-space T_1-weighted MRI images using the mutual information method of SPM8. Then, the T_1-weighted images were segmented into grey matter, white matter and CSF. The segmented grey matter images were spatially normalized into the Montreal Neurological Institute (MNI) grey matter provided by SPM8, and the inverse transformation matrix was used to label the segmented grey matter voxels in the patient's MRI-PET space according to a template of volumes of interest defined in the MNI space (Supplementary Fig. 1) (Berkouk *et al.*, 2006). For each volume of interest, partial volume effects-corrected, mean tracer concentrations were calculated for each participant. Briefly, segmented grey matter volumes of interest were corrected for the percentage of activity spilling from/to white matter whereas the CSF was constrained to zero because CSF is supposed to not have significant activity (Quarantelli *et al.*, 2004). Because the size of the sample was small, comparisons between Alzheimer's disease and healthy controls were performed using the Mann–Whitney U test. Alpha was set at 0.05 for all analyses.

In addition to using the arterial input function, we analysed the [^{11}C]-flumazenil PET data and compared the two groups using the pons as a reference region (Supplementary material).

Results

Neuropsychological performance

Patients with Alzheimer's disease had impaired memory. In addition, they performed significantly worse than healthy controls in some language tasks, but not on executive function tasks (Table 2).

Volumetric magnetic resonance imaging

On volume of interest analysis, hippocampal volumes were smaller in the Alzheimer's disease group (Fig. 2, Supplementary Table 1 and Supplementary Fig. 2). Cortical thickness and voxel-based morphometry yielded several regions, including the left medial temporal area, with decreased volume in Alzheimer's disease at uncorrected $P < 0.005$, but none which survived corrected significance (Supplementary Table 2 and Supplementary Figs 3 and 4). All the voxel-based, parametric contrasts, are displayed at the same *P*-value, to facilitate comparison across imaging modalities.

[^{18}F]-Fluorodeoxyglucose positron emission tomography

Left parietal association cortex and both precunei showed lower metabolism in Alzheimer's disease ($P < 0.005$ uncorrected), but none of these comparisons survived corrected significance (Supplementary Table 3 and Supplementary Fig. 5).

[^{11}C]-Flumazenil positron emission tomography

With voxel-based parametric analysis using arterial input function, flumazenil binding in patients with Alzheimer's disease was decreased in the left medial temporal region, including entorhinal cortex (whole brain analysis, cluster-level FWE-corrected $P = 0.048$; volume of interest, voxel-level FWE-corrected $P = 0.023$); and with uncorrected significance (voxel level $P < 0.005$), there was decreased binding in the right inferomedial temporal region, left precuneus and supramarginal gyri of both hemispheres (Fig. 1 and Table 3). With volume of interest analysis, [^{11}C]-flumazenil binding was decreased ($P < 0.05$) bilaterally in hippocampi and in the posterior cingulate gyrus (Supplementary Table 4 and Supplementary Fig. 6). Unlike with volumetric MRI, no false positives were recorded with [^{11}C]-flumazenil binding (Fig. 2). Hippocampal [^{11}C]-flumazenil binding correlated positively with measures of memory and other cognitive functions (Table 2 and Supplementary Fig. 7).

With the analysis using the pons as reference region, no regions were identified reaching corrected significance on voxel-based testing (Supplementary Table 5) or in volume of interest analysis (Supplementary Table 6). However, in voxel-based testing, regions that differed across groups were detected at the uncorrected $P < 0.005$ voxel level, largest in the left medial temporal region (Supplementary Table 5 and Supplementary Fig. 8) that were very similar to the ones detected with the arterial input method.

Discussion

We found [^{11}C]-flumazenil binding to be decreased in regions which, on extensive histological sampling, have shown the greatest degree of neuronal loss in early Alzheimer's disease. In a classical study, Brun and Englund (1981) found most marked neuronal loss in the medial temporal region, where [^{11}C]-flumazenil binding was most decreased in our study, but also in the posterior cingulate gyrus and in the supramarginal gyri of both hemispheres, regions with a strong trend for decreased [^{11}C]-flumazenil binding on voxel-based imaging (Supplementary Fig. 9), and in the case of the posterior cingulate, significantly lower for Alzheimer's disease in volume of interest analysis (Supplementary Table 4 and Supplementary Fig. 6).

In a study comparing [^{11}C]-flumazenil binding in older participants, two potential confounders were vascular disease and depression, both of which have been reported to lower [^{11}C]-flumazenil binding (Heiss *et al.*, 2004; Klumpers *et al.*, 2010). Vascular disease was carefully excluded from the Alzheimer's disease group, which served as a control for a different

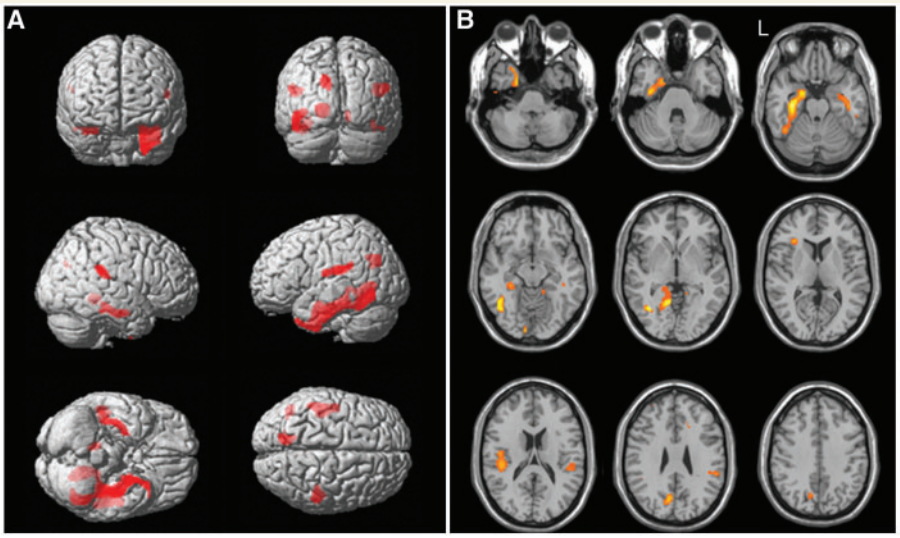

Figure 1 Regions where [^{11}C]-flumazenil binding was decreased in subjects with Alzheimer's disease compared to healthy controls (SPM8 voxel-based comparison, displayed at $P < 0.005$ uncorrected). Regions are displayed in red on rendered images of the brain surface (**A**) and in yellow-red on a standard axial template (**B**) using the neurological orientation (right hemisphere on the right side of each section). Note that in the medial temporal lobe, the findings reached corrected significance. The regions with decreased [^{11}C]-flumazenil binding are similar to the regions described as bearing the greatest degree of neuronal loss in classical neuropathological studies of early Alzheimer's disease (Supplementary Fig. 9).

[^{18}F]-fluorodeoxyglucose PET study (Pascual *et al.*, 2010), where Alzheimer's disease was compared with microvascular disease, the type of vascular disease most likely to be a confounder for this study. The depression rating scale score was higher in the group with Alzheimer's disease, although not significantly so and [^{11}C]-flumazenil binding correlated with depression scores (Table 2). However, we used the standard Geriatric Depression Scale to measure depression. Some of the items in this scale will be checked as positive not only in patients with depression, but also in those with cognitive impairment. For instance, the item that reads: 'Is your mind as clear as it used to be?' None of the patients with Alzheimer's disease had clinical depression.

We did not find significantly decreased binding in the posterolateral parietotemporal association cortex, where decreased metabolism is regularly seen in Alzheimer's disease (Chetelat *et al.*, 2008) and where an intermediate degree of neuronal loss was found by Brun and Englund (1981). Preserved [^{11}C]-flumazenil binding in this region may result from a delicate balance of neuronal loss versus increased expression of the $GABA_A$ receptor in the remaining neurons. Receptor plasticity has been documented after lesions of projection pathways. In rodents, lesions of the perforant hippocampal pathway resulted in an acute loss of GABA receptors, but similar levels to controls were recorded 30 days after the acute lesion (Mizukami *et al.*, 1997). A similar compensatory plasticity has been shown in Alzheimer's disease using post-mortem tissue. In the hippocampal formation, immunohistochemical, biochemical and *in situ* hybridization methods have shown an increased expression of $GABA_A$ receptors in the surviving neurons (Armstrong *et al.*, 2003; Iwakiri *et al.*, 2009). Similar data are not available for the posterior parietotemporal association cortex. While marked neuronal loss in medial temporal regions (Brun and Englund, 1981; Gomez-Isla *et al.*, 1996, 1997) would dictate that the total $GABA_A$ activity be reduced here, a milder loss in posterior parieto-temporal association cortex (Brun and Englund, 1981) may be compensated by an increase of $GABA_A$ receptors in the remaining neurons, leaving regional [^{11}C]-flumazenil binding unaltered, as we found in this region.

Several methodological differences may explain the positive finding in our study while previous studies of [^{11}C]-flumazenil in Alzheimer's disease, with a number of patients similar to ours, were negative (Meyer *et al.*, 1995; Ohyama *et al.*, 1999). First, we used voxel-based comparisons. By comparing all the voxels in the brain of patients with Alzheimer's disease and healthy controls, decreased binding can be found in areas that, when averaged with preserved areas in a volume of interest methodology, may pass undetected. In our study, apart from extensive changes in the medial temporal regions, other areas of decreased binding were small and likely to disappear when averaged with tissue containing normal binding values. For instance, despite decreased binding in both supramarginal gyri and the left precuneus (Fig. 1), overall binding in parietal lobes was not decreased in our volume of interest analysis (Supplementary Table 4 and Supplementary Fig. 6). Secondly, we used native space MRI to co-register it with native PET data and bring PET data to standard space. This technique not only allowed us to correct for partial volume effects, but also improved the quality of PET data in standard space and therefore the yield of all the comparisons performed across subjects and groups of subjects (Shan *et al.*, 2011). In addition, our subject samples were better matched by sex (Meyer *et al.*, 1995) and by age (Meyer *et al.*, 1995; Ohyama *et al.*, 1999).

Our findings agree with binding studies on Alzheimer's disease post-mortem tissue showing a 40% loss of benzodiazepine

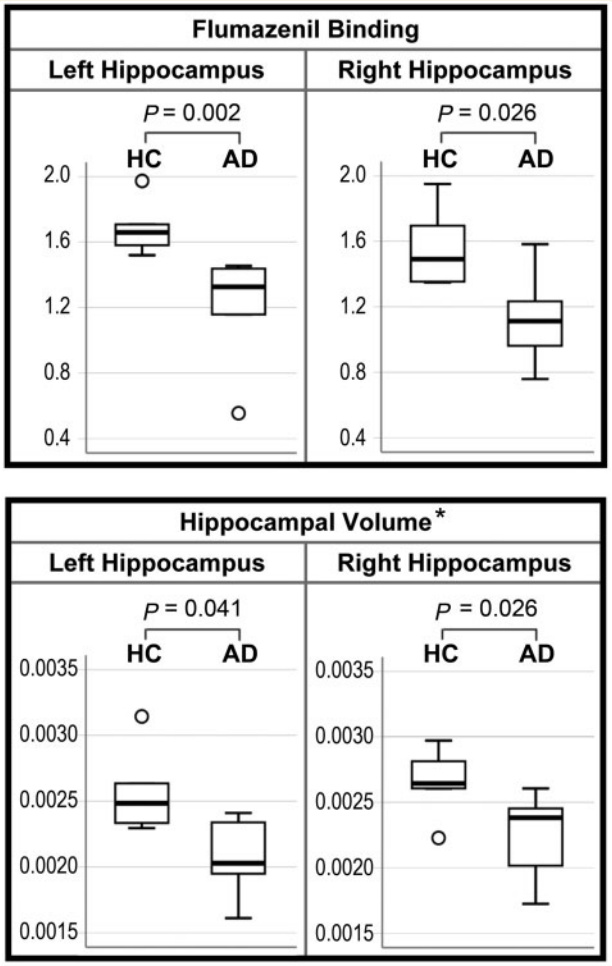

Figure 2 Box-and-whisker diagrams of partial volume effects-corrected hippocampal [^{11}C]-flumazenil binding (volume of distribution) and hippocampal volume (*ratio of individual hippocampal volume to individual whole-brain volume) in healthy controls (HC) and patients with Alzheimer's disease (AD). As customary, box boundaries represent quartiles, the thick line in the box is the median and the whiskers represent the samples minimum and maximum or, in the case of open circles, outliers. Statistical comparison was performed using the non-parametric Mann–Whitney *U* test.

binding in the entorhinal cortex (Jansen *et al.*, 1990) and variable losses of benzodiazepine or $GABA_A$ binding in the hippocampus and temporal cortex (Chu *et al.*, 1987; Shimohama *et al.*, 1988). As densitometric measurements on post-mortem tissue are confounded by artefactual volume loss, researchers working with tissue have often placed their findings in the context of *in vivo* receptor studies performed with PET and were cautious given the previously negative PET studies (Meyer *et al.*, 1995; Ohyama *et al.*, 1999). Our study, on the contrary, suggests that $GABA_A$ changes can be detected in early Alzheimer's disease using current imaging techniques. We studied early Alzheimer's disease because up to 40% of patients with mild cognitive impairment will not have prodromal Alzheimer's disease (Petersen, 2004). However, a quantification of hippocampal $GABA_A$ messenger RNA in post-mortem Alzheimer's disease and prodromal Alzheimer's disease–mild cognitive impairment tissue found a similar reduction of $GABA_A$ receptors at both stages of the disease (Rissman *et al.*, 2004), suggesting that it is worthwhile to look for changes in [^{11}C]-flumazenil binding in mild cognitive impairment or even preclinical stages.

Other than the hippocampal volumes on the volume of interest analysis, the findings on structural MRI did not reach corrected statistical significance. Given that structural MRI has proven useful in Alzheimer's disease and mild cognitive impairment (Misra *et al.*, 2009), the lack of significance in our study probably reflects the small sample size. Yet, the regions showing a trend for decreased volume were smaller but anatomically similar to areas showing decreased [^{11}C]-flumazenil binding (Supplementary Fig. 4). This finding supports the notion that decreased $GABA_A$ binding reflects neuronal loss (la Fougere *et al.*, 2011), which will also cause atrophy. However, the effect size for volume loss, both in the voxel-based analysis and the volume of interest analysis of volume (compare *r* values in Supplementary Tables 1 and 4), was smaller than for [^{11}C]-flumazenil binding loss.

[^{18}F]-Fluorodeoxyglucose PET showed a trend for decreased metabolism in the regions where this finding has been classically described in Alzheimer's disease (Chetelat *et al.*, 2008). A greater magnitude of neuronal loss, measured as decreased [^{11}C]-flumazenil binding, in the left medial temporal region (Fig. 1 and Table 3), corresponded to a greater loss of metabolism in the ipsilateral angular gyrus and retrosplenial region (Supplementary Fig. 5). This finding supports the concept that loss of metabolic activity in parietal association cortex may result, at least in part, from a reduction in the rich projections reaching this region from inferomedial temporal cortex (Lavenex *et al.*, 2002; Munoz and Insausti, 2005). It also highlights the dissociation between neuronal loss and loss of metabolism that has been reflected in other studies by a regional dissociation between atrophy and metabolic loss (Chetelat *et al.*, 2008).

The applicability of [^{11}C]-flumazenil PET imaging to the study of large samples of patients with Alzheimer's disease and controls would be greatly limited by the need to obtain arterial sampling, which is an invasive procedure. Fortunately, reference region methods have been described that obviate the need for arterial sampling in order to obtain an input function (Hammers *et al.*, 2008; Mourik *et al.*, 2008; Klumpers *et al.*, 2008). In our study, using the pons as a reference region yielded intergroup differences in medial temporal regions and precuneus that were significant at the uncorrected $P < 0.005$ level, which compares favourably to studies of [^{11}C]-flumazenil PET binding in epilepsy (Hammers *et al.*, 2008) or depression (Klumpers *et al.*, 2012) using the pons as reference region. However, at the same threshold, the arterial input method provided larger and more significant regions on voxel-based analyses and a greater intergroup effect on volume of interest analyses (Fig. 1 and Table 3; Supplementary Fig. 8 and Supplementary Tables 4–6). This finding agrees with the dictum that the ideal input function should not contain specific binding. Although in smaller amounts than in the cortex, $GABA_A$ receptors are present in the pons, and therefore the presence of some specific binding in this region makes it less than ideal as a reference region (Delforge *et al.*, 1995). It is possible that using carotid pixel density as an input function may yield

Table 3 Regions of lower [^{11}C]-flumazenil binding in patients with Alzheimer's disease compared with healthy controls on the voxel-based SPM analysis (sorted by cluster-level FWE-corrected significance)

Area of between-group difference	Brodmann area(s)	Side	*k*	*t*	*Z*	*P*-value		Maxima voxel MNI coordinates		
						Cluster-level FWE-corrected	Voxel-level Uncorrected*	(*x*, *y*, *z*)		
Medial temporal lobe	28, 35, 36	L	1980	6.60	4.01	$P = 0.048$	$P < 0.000$ ($P = 0.023$** FWE-corrected)	−42,	−64,	−4
Supramarginal gyrus	39, 40	L	352	4.50	3.25	$P = 0.758$	$P < 0.001$	−46,	−28,	20
Infero-medial temporal lobe	28, 36	R	242	4.24	3.14	$P = 0.865$	$P < 0.001$	40,	−26,	18
Precuneus cortex	31	L	190	4.45	3.23	$P = 0.909$	$P < 0.001$	−14,	−72,	30
Supramarginal gyrus	39, 40	R	181	4.21	3.12	$P = 0.916$	$P < 0.001$	48,	−34,	22
Posterior parahippocampal gyrus	35, 36	R	60	3.86	2.95	$P = 0.985$	$P < 0.002$	12,	−40,	6
Anterior insular cortex	44	L	51	4.50	3.25	$P = 0.988$	$P < 0.001$	−34,	26,	8
Angular gyrus	39	R	27	3.68	2.86	$P = 0.994$	$P < 0.002$	46,	−68,	48

*Voxel-level uncorrected *P*-values are provided as is customary and to facilitate comparison with other techniques (Supplementary material) as most of the intergroup comparisons do not reach corrected significance.
**Corrected for a volume encompassing both temporal lobes, known to be the cortical regions with earliest neuronal loss.
FWE = family-wise error; SPM = Statistical Parametric Mapping.

findings even more similar to the arterial-input-function method, yet without the need for arterial sampling (Mourik *et al.*, 2008). Another potential drawback of using [^{11}C]-flumazenil is the short half-life of ^{11}C, which dictates that a cyclotron be available at the imaging site. To address this issue, flumazenil labelled with ^{18}F, an isotope with a longer half-life, is being readied for clinical use (Massaweh *et al.*, 2009; la Fougere *et al.*, 2011).

[^{11}C]-Flumazenil is not the only agent available to image $GABA_A$ receptors *in vivo*. [^{123}I]-Iomazenil, a partial agonist, has also been used to image $GABA_A$ receptors in Alzheimer's disease by means of single photon emission computed tomography. The two [^{123}I]-iomazenil studies in Alzheimer's disease were positive, but data on medial temporal binding, the region with the greatest neuronal loss, were not available (Soricelli *et al.*, 1996; Fukuchi *et al.*, 1997). The patients in both studies had a lower Mini-Mental State Examination score than in our study, 14.7 ± 2.3 in Soricelli *et al.* (1996), suggesting more advanced Alzheimer's disease than in our sample (Student's *t*-test, two-tailed, $P = 0.02$). A study of [^{123}I]-iomazenil in mild cognitive impairment has been negative (Pappata *et al.*, 2010). Our findings may encourage more research with this compound. However, because the methodologies differ substantially, it is outside the scope of this paper to discuss investigations performed with [^{123}I]-iomazenil.

Using a sample size similar to those in previous studies of [^{11}C]-flumazenil binding, but updated methodology, we were able to separate patients with early Alzheimer's disease from healthy controls. As the findings on [^{11}C]-flumazenil PET reached statistical significance in precisely the areas of the brain known to have greatest neuronal loss, this report may encourage larger studies, which could confirm the usefulness of [^{11}C]-flumazenil PET for the detection of neuronal loss in early clinical or even preclinical stages.

Acknowledgements

The patients and healthy controls who participated in this study are gratefully acknowledged. We thank Dr Karl Herholz for leadership and many important suggestions, Dr Bradford Dickerson for helpful suggestions, Ms Jaione Irigoyen for providing nursing care and Mr Shane Kippenhan for help with the MRI morphometric procedure.

Funding

The EC-FP6-project DiMI of the European Community [LSHB-CT-2005-512146], the 'Unión Temporal de Empresas (UTE): Centro de Investigación Médica Aplicada,' University of Navarra, the 'Fundación Mutua Madrileña', the Government of Navarra [13255308-53-GN], and the 'Centro de Investigación Biomédica en Red de Enfermedades Neurodegenerativas (CIBERNED) of the Spanish Ministry of Health.

Supplementary material

Supplementary material is available at *Brain* online.

References

Armstrong DM, Sheffield R, Mishizen-Eberz AJ, Carter TL, Rissman RA, Mizukami K, et al. Plasticity of glutamate and GABAA receptors in the hippocampus of patients with Alzheimer's disease. Cell Mol Neurobiol 2003; 23: 491–505.

Ashburner J. A fast diffeomorphic image registration algorithm. Neuroimage 2007; 38: 95–113.

Berkouk K, Quarantelli M, Prinster A, Landeau B, Alfano B, Baron JC. Mapping the relative contribution of gray matter activity vs. volume in brain PET: a new approach. J Neuroimaging 2006; 16: 224–35.

Brun A, Englund E. Regional pattern of degeneration in Alzheimer's disease: neuronal loss and histopathological grading. Histopathology 1981; 5: 549–64.

Chen K, Ayutyanont N, Langbaum JB, Fleisher AS, Reschke C, Lee W, et al. Characterizing Alzheimer's disease using a hypometabolic convergence index. Neuroimage 2011; 56: 52–60.

Chetelat G, Desgranges B, Landeau B, Mezenge F, Poline JB, de la Sayette V, et al. Direct voxel-based comparison between grey matter hypometabolism and atrophy in Alzheimer's disease. Brain 2008; 131: 60–71.

Chetelat G, Villemagne VL, Bourgeat P, Pike KE, Jones G, Ames D, et al. Relationship between atrophy and beta-amyloid deposition in Alzheimer disease. Ann Neurol 2010; 67: 317–24.

Chu DC, Penney JB Jr., Young AB. Cortical GABAB and GABAA receptors in Alzheimer's disease: a quantitative autoradiographic study. Neurology 1987; 37: 1454–9.

Crystal H, Dickson D, Fuld P, Masur D, Scott R, Mehler M, et al. Clinico-pathologic studies in dementia: nondemented subjects with pathologically confirmed Alzheimer's disease. Neurology 1988; 38: 1682–7.

Delforge J, Pappata S, Millet P, Samson Y, Bendriem B, Jobert A, et al. Quantification of benzodiazepine receptors in human brain using PET, [11C]flumazenil, and a single-experiment protocol. J Cereb Blood Flow Metab 1995; 15: 284–300.

Fukuchi K, Hashikawa K, Seike Y, Moriwaki H, Oku N, Ishida M, et al. Comparison of iodine-123-iomazenil SPECT and technetium-99 m-HMPAO-SPECT in Alzheimer's disease. J Nucl Med 1997; 38: 467–70.

Giannakopoulos P, Herrmann FR, Bussiere T, Bouras C, Kovari E, Perl DP, et al. Tangle and neuron numbers, but not amyloid load, predict cognitive status in Alzheimer's disease. Neurology 2003; 60: 1495–500.

Gomez-Isla T, Hollister R, West H, Mui S, Growdon JH, Petersen RC, et al. Neuronal loss correlates with but exceeds neurofibrillary tangles in Alzheimer's disease. Ann Neurol 1997; 41: 17–24.

Gomez-Isla T, Price JL, McKeel DW Jr., Morris JC, Growdon JH, Hyman BT. Profound loss of layer II entorhinal cortex neurons occurs in very mild Alzheimer's disease. J Neurosci 1996; 16: 4491–500.

Hammers A, Panagoda P, Heckemann RA, Kelsch W, Turkheimer FE, Brooks DJ, et al. [11C]Flumazenil PET in temporal lobe epilepsy: Do we need an arterial input function or kinetic modeling? J Cereb Blood Flow Metab 2008; 28: 207–16.

Heiss WD, Sobesky J, Smekal U, Kracht LW, Lehnhardt FG, Thiel A, et al. Probability of cortical infarction predicted by flumazenil binding and diffusion-weighted imaging signal intensity: a comparative positron emission tomography/magnetic resonance imaging study in early ischemic stroke. Stroke 2004; 35: 1892–8.

Innis RB, Cunningham VJ, Delforge J, Fujita M, Gjedde A, Gunn RN, et al. Consensus nomenclature for in vivo imaging of reversibly binding radioligands. J Cereb Blood Flow Metab 2007; 27: 1533–9.

Iwakiri M, Mizukami K, Ikonomovic MD, Ishikawa M, Abrahamson EE, DeKosky ST, et al. An immunohistochemical study of GABA A receptor gamma subunits in Alzheimer's disease hippocampus: relationship to neurofibrillary tangle progression. Neuropathology 2009; 29: 263–9.

Jansen KL, Faull RL, Dragunow M, Synek BL. Alzheimer's disease: changes in hippocampal *N*-methyl-D-aspartate, quisqualate, neurotensin, adenosine, benzodiazepine, serotonin and opioid receptors—an autoradiographic study. Neuroscience 1990; 39: 613–27.

Kalbe E, Kessler J, Calabrese P, Smith R, Passmore AP, Brand M, et al. DemTect: a new, sensitive cognitive screening test to support the diagnosis of mild cognitive impairment and early dementia. Int J Geriatr Psychiatry 2004; 19: 136–43.

Killiany RJ, Gomez-Isla T, Moss M, Kikinis R, Sandor T, Jolesz F, et al. Use of structural magnetic resonance imaging to predict who will get Alzheimer's disease. Ann Neurol 2000; 47: 430–9.

Kisvarday ZF, Gulyas A, Beroukas D, North JB, Chubb IW, Somogyi P. Synapses, axonal and dendritic patterns of GABA-immunoreactive neurons in human cerebral cortex. Brain 1990; 113 (Pt 3): 793–812.

Klumpers UM, Boellaard R, Veltman DJ, Kloet RW, Hoogendijk WJ, Lammertsma AA. Parametric [11C]flumazenil images. Nucl Med Commun 2012; 33: 422–30.

Klumpers UM, Veltman DJ, Boellaard R, Comans EF, Zuketto C, Yaqub M, et al. Comparison of plasma input and reference tissue models for analysing [(11)C]flumazenil studies. J Cereb Blood Flow Metab 2008; 28: 579–87.

Klumpers UM, Veltman DJ, Drent ML, Boellaard R, Comans EF, Meynen G, et al. Reduced parahippocampal and lateral temporal GABAA-[11C]flumazenil binding in major depression: preliminary results. Eur J Nucl Med Mol Imaging 2010; 37: 565–74.

la Fougere C, Grant S, Kostikov A, Schirrmacher R, Gravel P, Schipper HM, et al. Where in-vivo imaging meets cytoarchitectonics: the relationship between cortical thickness and neuronal density measured with high-resolution [F-18]flumazenil-PET. Neuroimage 2011; 56: 951–60.

Lavenex P, Suzuki WA, Amaral DG. Perirhinal and parahippocampal cortices of the macaque monkey: projections to the neocortex. J Comp Neurol 2002; 447: 394–420.

Massaweh G, Schirrmacher E, la Fougere C, Kovacevic M, Wangler C, Jolly D, et al. Improved work-up procedure for the production of [(18)F]flumazenil and first results of its use with a high-resolution research tomograph in human stroke. Nucl Med Biol 2009; 36: 721–7.

McKhann G, Drachman D, Folstein M, Katzman R, Price D, Stadlan EM. Clinical diagnosis of Alzheimer's disease: report of the NINCDS-ADRDA Work Group under the auspices of Department of Health and Human Services Task Force on Alzheimer's Disease. Neurology 1984; 34: 939–44.

Meyer M, Koeppe RA, Frey KA, Foster NL, Kuhl DE. Positron emission tomography measures of benzodiazepine binding in Alzheimer's disease. Arch Neurol 1995; 52: 314–7.

Misra C, Fan Y, Davatzikos C. Baseline and longitudinal patterns of brain atrophy in MCI patients, and their use in prediction of short-term conversion to AD: results from ADNI. Neuroimage 2009; 44: 1415–22.

Mizukami K, Ikonomovic MD, Mishizen A, Sheffield R, Grayson DR, Armstrong DM. Alterations of GABA(A)beta2/3 immunoreactivity in the dentate gyrus after perforant pathway lesion. Neuroreport 1997; 8: 3379–83.

Mourik JE, Lubberink M, Klumpers UM, Comans EF, Lammertsma AA, Boellaard R. Partial volume corrected image derived input functions for dynamic PET brain studies: methodology and validation for [11C]flumazenil. Neuroimage 2008; 39: 1041–50.

Munoz M, Insausti R. Cortical efferents of the entorhinal cortex and the adjacent parahippocampal region in the monkey (*Macaca fascicularis*). Eur J Neurosci 2005; 22: 1368–88.

Ohyama M, Senda M, Ishiwata K, Kitamura S, Mishina M, Ishii K, et al. Preserved benzodiazepine receptors in Alzheimer's disease measured with C-11 flumazenil PET and I-123 iomazenil SPECT in comparison with CBF. Ann Nucl Med 1999; 13: 309–15.

Okazawa H, Yamauchi H, Sugimoto K, Magata Y, Kudo T, Yonekura Y. Effects of metabolite correction for arterial input function on quantitative receptor images with 11C-flumazenil in clinical positron emission tomography studies. J Comput Assist Tomogr 2004; 28: 428–35.

Pappata S, Varrone A, Vicidomini C, Milan G, De Falco C, Sansone V, et al. SPECT imaging of GABA(A)/benzodiazepine receptors and cerebral perfusion in mild cognitive impairment. Eur J Nucl Med Mol Imaging 2010; 37: 1156–63.

Pascual B, Prieto E, Arbizu J, Marti-Climent J, Olier J, Masdeu JC. Brain glucose metabolism in vascular white matter disease with dementia: differentiation from Alzheimer disease. Stroke 2010; 41: 2889–93.

Petersen RC. Mild cognitive impairment as a diagnostic entity. J Intern Med 2004; 256: 183–94.

Prieto E, Marti-Climent JM, Arbizu J, Garrastachu P, Dominguez I, Quincoces G, et al. Evaluation of spatial resolution of a PET scanner through the simulation and experimental measurement of the recovery coefficient. Comp Biol Med 2010; 40: 75–80.

Quarantelli M, Berkouk K, Prinster A, Landeau B, Svarer C, Balkay L, et al. Integrated software for the analysis of brain PET/SPECT studies with partial-volume-effect correction. J Nucl Med 2004; 45: 192–201.

Rissman RA, Bennett DA, Armstrong DM. Subregional analysis of GABA(A) receptor subunit mRNAs in the hippocampus of older

persons with and without cognitive impairment. J Chem Neuroanat 2004; 28: 17–25.

Rocher AB, Chapon F, Blaizot X, Baron JC, Chavoix C. Resting-state brain glucose utilization as measured by PET is directly related to regional synaptophysin levels: a study in baboons. Neuroimage 2003; 20: 1894–8.

Rousset OG, Ma Y, Evans AC. Correction for partial volume effects in PET: principle and validation. J Nucl Med 1998; 39: 904–11.

Sedvall G, Nyback H, Farde L, Persson A. Neurotransmitter receptor imaging in Alzheimer's disease. J Neural Transm Suppl 1987; 24: 43–8.

Shan ZY, Mateja SJ, Reddick WE, Glass JO, Shulkin BL. Retrospective evaluation of PET-MRI registration algorithms. J Digit Imaging 2011; 24: 485–93.

Shimohama S, Taniguchi T, Fujiwara M, Kameyama M. Changes in benzodiazepine receptors in Alzheimer-type dementia. Ann Neurol 1988; 23: 404–6.

Soricelli A, Postiglione A, Grivet-Fojaja MR, Mainenti PP, Discepolo A, Varrone A, et al. Reduced cortical distribution volume of iodine-123 iomazenil in Alzheimer's disease as a measure of loss of synapses. Eur J Nucl Med 1996; 23: 1323–8.